# Complexes between Chaperonin GroEL and the Capsid Protein of Bacteriophage HK97†

Yuan-hua Ding, Robert L. Duda, Roger W. Hendrix, and John M. Rosenberg*

*Department of Biological Sciences, University of Pittsburgh, Pittsburgh, Pennsylvania 15260*

*Received June 14, 1995; Revised Manuscript Received September 14, 1995*®

ABSTRACT: The 42 kDa capsid protein of bacteriophage HK97 requires the GroEL and GroES chaperonin proteins of its *Escherichia coli* host to facilitate correct folding, both *in vivo* and *in vitro*. In the absence of GroES and ATP, denatured gp5 forms a stable complex with the 14 subunit GroEL molecule. We characterized the electrophoretic and biochemical properties of this complex. In electrophoresis on a native (nondenaturing) gel, the band of the gp5−GroEL complex shifts to a slower migrating position relative to uncomplexed GroEL. The results show that there is only one subunit of gp5 bound to each GroEL 14-mer and that the shift in band position is due primarily to a change in the overall charge of the complex relative to uncomplexed GroEL, and not to a change in size or shape. GroEL forms similar complexes with proteolytic fragments of gp5, with a series of sequence duplication derivatives of gp5, and with other proteins. Electrophoretic examination of these complexes shows that a band shift occurs with proteins larger than 31−33 kDa but not with smaller proteins. For those proteins that cause a band shift upon complex formation, the magnitude of the shift is correlated with the predicted negative charge on the protein; paradoxically, the direction of the band shift is opposite to what is predicted if the charge of the complex were simply the sum of the charge of GroEL and the charge of the substrate protein. We suggest that binding of a substrate protein to GroEL is accompanied by a net binding of solution cations to the complex, but only in the case of proteins above a minimum size of 31−33 kDa. The gp5−GroEL complex is in an association/dissoication equilibrium, with a binding constant measured in the range of 11−17 $\mu M^{-1}$.

The primary amino acid sequence of a protein solely determines its unique secondary and tertiary structure, and, for most proteins, spontaneous refolding *in vitro* can lead to their native conformation given the appropriate solution conditions (Anfinsen, 1973). But for many other proteins, spontaneous refolding in free solution is not successful because irreversible aggregation of folding intermediates will greatly reduce, if not completely eliminate, the yield of the native structure (Viitanen et al., 1992). The effective folding of most *Escherichia coli* proteins, both *in vivo* and *in vitro*, requires their association with a family of accessory proteins called chaperones (Ellis et al., 1991; Viitanen et al., 1992; Georgopoulos et al., 1993). Chaperones are abundant and indispensable proteins that are involved in the posttranslational folding and transport of newly synthesized protein in the cell (Ellis, 1991; Viitanen et al., 1992; Georgopoulos et al., 1993). Functions suggested for chaperones include binding to partially folded intermediates of a peptide, mainly through hydrophobic interactions, to prevent them from self-aggregation and from folding into incorrect conformations (Ellis et al., 1991). Among chaperones, two members of the chaperonin subfamily from *E. coli*, Cpn60 (GroEL) and its cofactor, Cpn10 (GroES), have been studied extensively (Georgopoulos et al., 1993).

GroEL is composed of 14 identical subunits of about 60 kDa arranged in 2 stacked heptameric rings (Hendrix, 1979; Hohn et al., 1979; Chen et al., 1994; Braig et al., 1994). It is a $K^+$-dependent weak ATPase (Hendrix, 1979; Viitanen et al., 1990; Todd et al., 1993). There are $Mg^{2+}$ and adenosine nucleotide binding sites on each subunit of GroEL. GroES exists as single homo-heptameric ring of 10 kDa subunits (Tilly et al., 1981; Chandrasekhar et al., 1986). In the presence of $Mg^{2+}$ and adenosine nucleotide, GroES forms a stable complex with GroEL and inhibits the ATPase of GroEL (Chandrasekhar et al., 1986; Saibil et al., 1992; Ishii et al., 1992; Chen et al., 1994). It has been suggested that the substrate peptide is bound in the central cavity formed by the heptameric rings of GroEL (Braig et al., 1993; Chen et al., 1994). Binding to GroEL alone is capable of arresting the spontaneous refolding and self-aggregation of the substrate protein (Viitanen et al., 1992). Upon discharge from GroEL, which usually requires both GroES and $Mg^{2+}$−ATP, the substrate protein is left partially unfolded and partitions between "committed" and "kinetically trapped" intermediates (Todd et al., 1994). The former will lead to the native structure, while the latter will be rebound to GroEL and recycled again (Todd et al., 1994).

Knowledge of the structural features of the substrate protein which are responsible for its interaction with GroEL is important for the understanding of GroEL-facilitated protein folding. GroEL forms stable complexes with the folding intermediates but not the native forms of a number of proteins (Evers et al., 1992; Fisher, 1992; Mendoza et al., 1992). GroEL may recognize structural features which are not present in the native structure, mainly exposed hydrophobic surfaces.

† This work was supported by NIH Grants GM47795 (R.W.H.) and GM25671 and RR10447 (J.M.R.) from the U.S. Public Health Service.

* Author to whom correspondence should be addressed. Telephone: 412-624-4636. Fax: 412-624-4759.

® Abstract published in *Advance ACS Abstracts,* November 1, 1995.

0006-2960/95/0434-14918$09.00/0 

HK97 is a lambdoid bacteriophage of *Escherichia coli* that is shown to be a useful experimental system for investigating viral assembly (Duda et al., 1995a,b). Previous genetic experiments show that the *E. coli* GroEL gene is required for the assembly of heads or head-related structures in HK97-infected cells (Popa, 1988). *In vitro* protein folding experiments have shown that GroEL, GroES, and $Mg^{2+}$−ATP are required for the effective folding of the 42 kDa major head protein of bacteriophage HK97, gp5 (Xie & Hendrix, 1995). GroEL and gp5 form a stable complex which can be separated from the uncomplexed proteins by gel filtration and glycerol gradient centrifugation. The gp5−GroEL complex shows a characteristic band shift in either agarose gels or low percentage native polyacrylamide gels. In this paper, we investigate the origin of the band shift in native gel electrophoresis caused by gp5 binding and attempt to elucidate the mechanism of interaction between GroEL and its substrate polypeptides.

## MATERIALS AND METHODS

*Buffer.* All experiments, unless otherwise specified, were carried out in TKG buffer with 10 mM Tris-HCl, pH 7.0, 50 mM potassium glutamate, 0.1 mM EDTA, and 0.1% 2-mercaptoethanol (v/v).

*Expression and Purification of Proteins. (A) GroEL and GroES Proteins.* GroEL and GroES proteins were purified from an *E. coli* strain that carries the plasmid pOF39 (Fayet et al., 1986) as described in Hendrix (1979) and Chandrasekhar et al. (1986). Purified GroEL and GroES were concentrated to at least 15 mg/mL using the Centricon 100 and Centricon 30 centrifugal filtration concentrators (Amicon), respectively. Both proteins were stored in TKG buffer with 20% glycerol at −20 °C.

*(B) HK97 (Prohead I).* HK97 head protein, gp5, in the prohead I form was purified from an *E. coli* strain with a plasmid containing the HK97 head protein gene using methods modified from a previous report (Duda et al., 1995b). The amino acid sequence of HK97 gp5 was reported in Duda et al. (1995a,b). Cells were grown to $3 \times 10^8$ cells/mL at 37 °C, induced with 0.4 mM IPTG for 2 h, harvested, and resuspended in 50 mM Tris-HCl, pH 8.0, with 5 mM EDTA. Cells were lysed with 50 μg/mL lysozyme (from freshly made stock, 1.0 mg/mL) and treated with DNase I (to 20 μg/mL aiong with 7.5 mM $MgSO_4$). Cell debris was removed by centrifugation, and proheads in the lysate supernatant were precipitated by the addition of 0.15 M KCl and 10% PEG 8000 (w/v). The pellet was resuspended in TKG and pelleted by centrifugation in a Beckman Ti45 rotor at 35K rpm for 2 h at 4 °C. The ultracentrifugal pellet was overlaid with TKG buffer, left overnight to resuspend, and loaded onto a 35 mL 10−30% glycerol step gradient. The centrifugation was carried out in a Beckman SW28 rotor for about 2.5 h at 24K rpm at 4 °C. The proheads formed a single visible band in the gradient which was extracted from the side of the centrifuge tube with a syringe. The extracted band was diluted with TKG and concentrated by sedimentation in a Beckman Ti45 rotor as described above.

The cleaved gp5, gp5* (31 kDa), was purified in the prohead II form by a protocol similar to that described above for prohead I (Duda et al., 1995b).

*(C) Preparation of 24 and 18 kDa Tryptic Digestion Fragments of gp5.* The preparation of N-terminal 18 kDa and C-terminal 24 kDa tryptic digestion fragments of gp5 was done using a protocol developed by Zhihua Xie (Xie, 1994). Purified prohead I (20 mg/mL in TKG) was treated with trypsin (25 μg/mL) overnight. Analysis on an SDS gel shows that gp5 is cleaved quantitatively into two fragments: an N-terminal 18 kDa fragment, and a C-terminal 24 kDa fragment. The cleaved proheads were precipitated with 10% TCA, washed with ice-cold acetone, and dissolved in 3.5 M guanidinium chloride (GuHCl). The unfolded protein produced was diluted at room temperature into TKG buffer by quickly mixing 1 part protein with 20 parts TKG. The C-terminal 24 kDa fragments aggregate, while the N-terminal 18 kDa fragments remain soluble. The diluted protein was centrifuged for 30 min, and the resulting precipitate, which contained only the C-terminal 24 kDa fragment, was washed once with TKG to remove residual supernatant and redissolved in 3.5 M GuHCl. The supernatant, which contained the N-terminal 18 kDa fragment exclusively, was precipitated by adding TCA to 10%. The pellet was washed with acetone and redissolved in 3.5 M GuHCl.

*(D) Mutant Forms of the HK97 Virus Head Protein.* Several variants of the HK97 gene 5 protein that contain internal duplications were used in this study and are described in Figure 4. The proteins encoded by HK97 gene 5 duplication mutants dm1, dm8, dm9, dm11, dm12, dm13, dm14, dm15, dm16, and dm17 all form inclusion bodies when expressed in *E. coli* at 37 °C. The cells were grown and induced as for wild-type prohead I described above. The cells were lysed by sonication using a microtip horn on a Branson Sonifier (Model 250) and the lysates centrifuged at 14000*g*. The lysate pellets, which contain most of the mutant proteins, were resuspended in TKG by sonication and recentrifuged. The pellets were washed as above with one cycle of 1.5 M KCl in TKG, one cycle of TKG, one cycle of TKG containing 0.1% *n*-octyl glucoside (w/v), and another cycle of TKG. The mutant proteins in the final pellets were estimated to be 95% pure.

The HK97 gene 5 duplication mutant dm6, which forms proheads (K. Martincic and R. Hendrix, unpublished data), was purified as described above for wild-type prohead I.

*(E) Purification of [$^{35}$S]Methionine-Labeled GroEL Protein.* GroEL protein was labeled with L-[$^{35}$S]methionine *in vivo*. Cells were grown to $3 \times 10^8$ cells/mL at 37 °C in 50 mL of RG glucose medium (an M9-derived minimal labeling medium; Georgopoulos et al., 1973) and transferred to 42 °C. At 30 and 40 min after the heat shock, 1 μCi/mL L-[$^{35}$S]-methionine (New England Nuclear) was added to the medium. Cells were grown for another hour and harvested by centrifugation. The cells were resuspended on ice in 50 mM Tris-HCl, pH 8.0, with 5 mM EDTA. Lysozyme (from a fresh stock solution) was added to about 50 μg/mL, and the suspension was incubated on ice for about 1 h. Following lysis, $MgSO_4$ (to 7.5 mM from a 1 M stock) and DNase I (to 20 μg/mL from a 1 mg/mL stock) were added followed by further incubation to reduce the viscosity of the lysate. The cell debris was removed by centrifugation, and the GroEL protein in the supernatant was purified by velocity sedimentation in a 10−30% glycerol gradient. Gradient fractions containing GroEL were pooled and loaded onto a DEAE-cellulose column (Whatman DE52) equilibrated with 10 mM Tris-HCl, pH 7.5, and 0.1 M NaCl. The column was eluted with a 0.1−0.5 M NaCl gradient. GroEL fractions were collected and concentrated using a Centricon 100 centrifugal filtration concentrator.

*(F) Purification of [$^{35}$S]Methionine-Labeled HK97 Prohead I and dm11 Proteins.* *E. coli* strains containing plasmids that overexpress wild-type gp5 or dm11 protein were labeled with L-[$^{35}$S]methionine as described (Duda et al., 1995a). Labeled gp5 was purified as described above. Labeled dm11 was purified similarly to unlabeled dm11 except that the cells were lysed with lysozyme.

*(G)* The P22 virus was purified by the method of Earnshaw et al. (1976). *Eco*RI endonuclease was purified by the method of Greene (Greene et al., 1974). Tumor-associated aldehyde dehydrogenase (ALDH) from rat *(Rattus norvegicus)* was a gift from Dr. John Hempel in the Department of Biochemistry and Molecular Genetics, University of Pittsburgh (Jones et al., 1988). RepC protein from *Staphylococcus aureus* was a gift from Dr. Saleem Khan from the same department (Novick et al., 1982).

*Formation of the GroEL−Substrate Complex.* Past experiments show that neither the time of exposure to GuHCl (1 h to overnight or even longer) nor the GuHCl concentration (3.5−7 M) affects the final binding of and GroEL-assisted refolding of gp5. In this report, we denatured the protein in 3.5 M GuHCl and renatured it by dilution of 1 volume of denatured protein into 20 volumes of GroEL solution to give a final GuHCl concentration of 0.17 M. Unless otherwise specified, the initial substrate protein concentration (after dilution) in the GroEL solution was 4-fold higher than that of the GroEL 14-mer. The complex solution was stored at room temperature, unless specified, for 30 min, and then centrifuged at 14000*g* at 4 °C for 30 min to remove aggregates.

*Gel Electrophoresis. (1) Agarose Gel Electrophoresis.* Native agarose gel electrophoresis was done as described for the study of viral and other large protein assemblies (Duda et al., 1995b). Samples were electrophoresed in TAMg buffer (Tris−acetate−magnesium sulfate). Samples for electrophoresis were prepared by mixing 9 parts sample with 1 part agarose gel sample buffer [50% (v/v) glycerol, 0.025% (w/v) bromphenol blue, and 0.025% (w/v) xylene cyanol XFF]. The gel was electrophoresed at 80−100 V for about 2 h at room temperature. After electrophoresis, the gel was fixed [25% (v/v) 2-propanol and 10% (v/v) acetic acid, 20 min], equilibrated with 95% ethanol (v/v in water), and dried. The dried gel was stained with Coomassie brilliant blue R-250 and redried onto filter paper as for a polyacrylamide gel.

*(2) SDS−Polyacrylamide Gel Electrophoresis (SDS−PAGE).* The methods and conditions for SDS−PAGE were modified from Laemmli (1970). All samples were heated in boiling water for 3 min after mixing 3 parts sample with 1 part 4× SDS sample buffer [0.25 M Tris-HCl, pH 6.8, 8% (w/v) SDS, 20% 2-mercaptoethanol, 20% glycerol, and 0.025% (w/v) bromphenol blue]. The gel was stained with Coomassie brilliant blue R-250.

*(3) Native Polyacrylamide Gel Electrophoresis (Native PAGE).* Native polyacrylamide gel electrophoresis conditions were modified from Ornstein and Davis (1964). In refolding assay solutions, the concentration of GuHCL is 0.17 M, an ionic strength sufficiently high to make the stacking gel lose stacking capability under the usual conditions for discontinuous electrophoresis. This was resolved by adjusting buffer concentrations and adding extra salt to the stacking gel, the running gel, and the electrode buffer. The final Tris-HCl concentration in the stacking gel was 150 mM, pH 6.8, and contained up to 30 mM KCl. The final Tris-HCl concentration in the running gel is 750 mM, pH 8.8, and contained up to 70 mM KCl. The electrode buffer contained 25 mM Tris base, 0.19 M glycine, and 20 mM KCl. Samples for native PAGE electrophoresis were prepared by mixing 3 parts sample with 1 part 4× native PAGE sample buffer. Native sample buffer is identical to the 4× SDS−PAGE sample buffer, but without SDS. Because of the high ionic strength in the native PAGE system, the gel was run at 40−50 V for a period of 4 h. The gel was stained with Coomassie brilliant blue R-250 as described for SDS−PAGE.

*Scanning of Stained Wet Gel.* Wet and well-destained polyacrylamide gels were scanned in the 2D mode by a Zeineh soft laser scanning densitometer (Biomed Instruments, Inc., Model SLR-2D/1D). The data were analyzed by the "ZEINEH 2-D PCI XVII Program IBM pc" program on an IBM personal computer.

*Scanning of Gels with Radioactive Proteins.* Gels with L-[$^{35}$S]methionine-labeled proteins were dried onto filter paper, flattened, scanned, and then analyzed on an AMBIS 400 Image Acquisition and Analysis System (Ambis, Inc.).

*Refolding of gp5 from the GroEL Complex.* 600 $\mu$L of 0.8 $\mu$M GroEL 14-mer was complexed with denatured [$^{35}$S]-methionine-labeled gp5 as described above. To initiate refolding, 15 mM $Mg^{2+}$−ATP (4.8 $\mu$L) and 3.0 $\mu$M GroES (15.2 $\mu$L) were added to 40 $\mu$L of preformed complex to obtain 1.2 mM $Mg^{2+}$−ATP and 0.76 $\mu$M GroES at a final volume of 60 $\mu$L. In control experiments, an equal volume of TKG was added in place of $Mg^{2+}$−ATP or GroES. GroES and $Mg^{2+}$−ATP were added at various times to give reaction times (the time from refolding initiation until electrophoresis began) of 1, 2, 4, 6, 8, 15, 20, 30, 40, and 60 min. For the control without GroES or $Mg^{2+}$−ATP, the incubation time was 60 min. To stop refolding, samples were mixed with 40 mM EDTA in 15 $\mu$L of 4× native PAGE sample buffer and run on a 5% native polyacrylamide gel.

*Ferguson Analysis.* Samples of 1 mg/mL HK97 prohead I, 1 $\mu$M free GroEL with 0.17 M GuHCl, and 1 $\mu$M GroEL−gp5 complex were loaded onto a series of gels of different agarose percentages (0.8%, 1.0%, 1.2%, 1.4%, 1.6%, 1.8%, 2.0%, 2.2%, 2.4%) and electrophoresed at 100 V. After electrophoresis, the gels were marked with small holes at the dye front position and processed as previously described. The distance $R$, each individual component migrated (the distance between the loading well and the center line of the corresponding band) was measured. The distance from the loading well to the dye front was also measured, and the relative mobility ($R_f$ = distance migrated by protein/distance migrated by dye) was calculated. A Ferguson plot (Hames, 1981), log($R_f$) against the percentage of agarose (T%), was constructed from these data.

*Stoichiometry of GroEL−gp5 Complex.* Concentrations of gp5 and GroEL were both determined by quantitative amino acid analysis. Samples were hydrolyzed in vacuo at 110 °C for 27 h and analyzed using a Beckman 6300 amino acid analyzer (Beckman Instruments, Fullerton, CA). Unlabeled prohead I, [$^{35}$S]methionine-labeled prohead I, unlabeled dm11 protein, and [$^{35}$S]methionine-labeled dm11 protein were adjusted to the same concentration and denatured in 3.5 M GuHCl. One part of denatured [$^{35}$S]-methionine-labeled gp5 was mixed with 1 part of denatured unlabeled dm11 protein to make a [$^{35}$S]methionine-labeled gp5−unlabeled dm11 mixture. Similarly, 1 part of unlabeled gp5 was mixed with 1 part of [$^{35}$S]methionine-labeled dm11.

Four kinds of complex were formed: GroEL with [$^{35}$S]-methionine-labeled gp5, GroEL with [$^{35}$S]methionine-labeled dm11, GroEL with [$^{35}$S]methionine-labeled gp5 and unlabeled dm11 protein, and GroEL with unlabeled gp5 and [$^{35}$S]-methionine labeled dm11 protein. The resulting four complexes were analyzed by native PAGE as described. The gel was stained, dried, and radioautographed.

*Trypsin Digestion of gp5 Bound to GroEL.* The GroEL−gp5 complex was formed by diluting denatured [$^{35}$S]-methionine-labeled HK97 prohead I (gp5) into 1660 μL of 0.26 μM GroEL 14-mer and divided into 200 μL aliquots. Digestion was initiated with 10 μg/mL trypsin (from a 250 μg/mL stock) to each aliquot to give digestion times of 7.5, 15, 30, 45, 60, 90, and 120 min. Digestion was stopped with 4 μL of phenylmethanesulfonyl fluoride (PMSF, 100 mM dissolved in ethyl alcohol; Sigma) followed by the addition of a 10 μL mixture of soybean trypsin inhibitor (8 mg/mL stock, Sigma) and $N^{\alpha}$-*p*-tosyl-L-lysine chloromethyl ketone (TLCK) (0.1 mg/mL, Sigma). A fraction of the digested complex (40 μL) was mixed with 4X native PAGE sample buffer (15 μL) and loaded onto a 5% native polyacrylamide gel. The remainder was precipitated with 400 μL of 20% TCA, washed with ice-cold acetone, dissolved and heated in 100 μL of 1X SDS sample buffer, and run on an SDS−polyacrylamide gel. The gels were stained, photographed, and dried for autoradiography.

*Dissociation/Reassociation Equilibrium of the GroEL−gp5 Complex.* The GroEL−gp5 complex was formed using denatured gp5 and 150 μL of 0.8 μM GroEL as described above. To 30 μL of the complex (Figure 8, lane 5) was added 5 μL of 2.4 μM GroEL to capture any unbound gp5 in the complex solution. After 5 min, 5 μL of 2.4 μM [$^{35}$S]-methionine-labeled GroEL was added to measure the exchange of the [$^{35}$S]methionine-GroEL into the GroEL−gp5 complex. As a control, [$^{35}$S]methionine-GroEL and GroEL were also added (Figure 8, lane 4). To eliminate the possibility of trace contamination by GroES and $Mg^{2+}$−ATP, the complex solution and the [$^{35}$S]methionine-GroEL were both pretreated with EDTA (Figure 8, lane 6) as follows: 5 μL of 60 mM EDTA in 10 mM Tris-HCl, pH 7.5, and 5 μL of 2.4 μM GroEL were each added to 30 μL of complex; another 5 μL of EDTA was added to 5 μL of 2.4 μM [$^{35}$S]-methionine-GroEL. As controls, 30 μL of TKG was mixed with 1.5 μL of 3.5 M GuHCl (Figure 8, lane 1) or denatured gp5 in 3.5 M GuHCl (Figure 8, lane 2) and incubated for 30 min; 10 μL of 2.4 μM [$^{35}$S]methionine-GroEL and 10 μL of 2.4 μM GroEL were subsequently added. To ensure uniform gel conditions, the EDTA concentration in all samples was equivalent when loaded onto a native 5% native polyacrylamide gel.

*Measurement of Total Refoldable gp5 in the GroEL−gp5 Complex Solution.* The [$^{35}$S]methionine GroEL−gp5 complex was made from [$^{35}$S]methionine-labeled GroEL and denatured unlabeled gp5 as described above; 168 μL of this 0.266 μM [$^{35}$S]methionine-GroEL−gp5 complex was mixed with 56 μL of 4X native PAGE sample buffer to yield a final complex concentration of 0.2 μM. The complex was allowed to reach equilibrium at room temperature. A 4 μM [$^{35}$S]methionine-labeled GroEL stock solution was mixed with TKG and 4X native PAGE sample buffer to achieve resulting GroEL solutions containing 1X sample buffer and 0.8, 1.1, 1.4, 1.7, 2.0, 2.3, 2.6, and 3.2 μM [$^{35}$S]methionine-labeled GroEL. To 20 μL of each labeled solution was added 20 μL of the 0.2 μM GroEL complex to achieve final concentrations of 0.4, 0.5, 0.6, 0.7, 0.8, 0.9, 1.0, and 1.2 μM [$^{35}$S]methionine-labeled GroEL (sample 2−sample 9). The samples were incubated at room temperature for 20 min and analyzed on a 5% native PAGE. Samples 1 and 10 are the original 0.2 μM [$^{35}$S]methionine-GroEL−gp5 complex. A similar procedure was followed with the initial [$^{35}$S]-methionine-GroEL−gp5 complex at 0.4 μM. The gels were stained, dried, and scanned by the AMBIS radioanalytical imaging system for radioactivity. Data analysis is discussed in the legend of Figure 9 and below.

*Estimation of the Equilibrium Constant of the GroEL−gp5 Complex.* The total gp5 (both bound and unbound) in the initial GroEL−gp5 complex was estimated from the data presented in Figure 9. The initial complex solution was analyzed on a native polyacrylamide gel, and the ratio of complexed GroEL to free GroEL was calculated based on radioactivity measurements. Since one GroEL molecule can bind only one gp5 polypeptide, and since we know the total gp5 in the solution based on the concentration of complexed GroEL, we were able to calculate the amount of unbound gp5. From this, the equilibrium constant was calculated.

We consider the case of an initial concentration of 0.20 μM GroEL−gp5 complex. We assume that when enough free GroEL is added, all of the gp5 will be in the complex form. From Figure 9, when GroEL was added to 1.2 μM, the concentration of GroEL−gp5 complex was 0.17 μM. So, the total gp5 in this condition was 0.17 μM too. Then for the initial 0.20 μM GroEL−gp5 complex solution, the total gp5 concentration is $0.17 \times 1.5 = 0.26$ μM (using a factor of 1.5 to correct for diultion because 20 μL of 0.20 μM GroEL−gp5 complex was mixed with 10 μL of 3.2 μM free GroEL to get 1.2 μM GroEL−gp5 complex solution). The gp5-bound GroEL and the free GroEL in the initial 0.20 μM GroEL−gp5 complex solution were separated in the native polyacrylamide gel, and the concentrations of the two species were measured through radioactivity of [$^{35}$S]methionine-GroEL. The ratio of upper band counts to the sum of upper band counts and lower band counts is 0.62, so the concentration of GroEL in the complex form is 0.12 μM, and that of free GroEL is $0.20 - 0.12 = 0.08$ μM. Since the total [gp5] is 0.26 μM, the free [gp5] is $0.26 - 0.12 = 0.14$ μM. Thus, the binding constant is [GroEL−gp5 complex]/{[free GroEL] × [free gp5]} = $0.12/(0.08 \times 0.14) = 11$ $\mu M^{-1}$.

For the case of an initial 0.4 μM GroEL−gp5 complex, a similar experiment was done, and the binding constant was calculated to be about 17 $\mu M^{-1}$.

## RESULTS

*Binding of HK97 gp5 to GroEL Causes a Band Shift of GroEL in Native Gel Electrophoresis.* The chaperonin GroEL, together with the cofactors GroES and $Mg^{2+}$−ATP, can mediate the effective refolding *in vitro* of GuHCl-denatured HK97 head protein, gp5, into native hexamers and pentamers—intermediates in the pathway of the HK97 head assembly (Xie & Hendrix, 1995; Figure 1). In the absence of cofactors GroES and $Mg^{2+}$−ATP, GroEL forms a stable complex with gp5. Complex formation was demonstrated by cosedimentation of gp5 with GroEL during glycerol gradient sedimentation and coelution during size-exclusion chromatography (data not shown). The GroEL-bound gp5 remains refoldable at room temperature when GroES and $Mg^{2+}$−ATP are added within a period of 24 h after complex formation; the refolding yield gradually decreases if the complex is stored for longer periods.

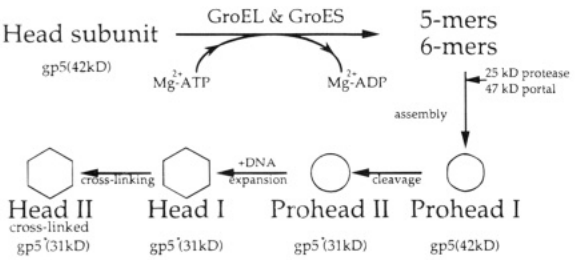


FIGURE 1: HK97 head assembly pathway (Duda et al., 1995a,b). The 42 kDa head subunit of HK97, gp5, folds and assembles into 5-mers and 6-mers with the assistance of the GroELS−$Mg^{2+}$−ATP system (Xie, 1994; Xie & Hendrix, 1995). The 5-mers and 6-mers, along with the viral protease and portal proteins assemble into prohead I. In the transition from prohead I to prohead II, each gp5 protein loses 102 amino acids from its N-terminus due to the action of the viral protease. DNA packaging triggers a conformational change of prohead II and causes its transition to head I. In head II, each of the major head subunits (gp5*) is covalently linked to its neighbors.

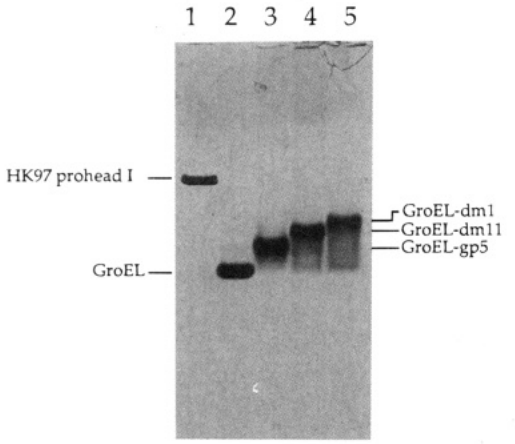


FIGURE 2: Substrates bound to GroEL cause an electrophoretic mobility shift of GroEL as shown in an agarose gel. Samples were run in a 1.6% agarose gel. Lane 1, HK97 prohead I; lane 2, GroEL; lane 3, the GroEL−gp5 complex; lane 4, the GroEL−dm11 complex; lane 5, the GroEL−dm1 complex. dm1 and dm11 are duplication mutations of the HK97 gp5 polypeptide (see Figure 4). In lanes 3−5, the smear below complex bands is due to the dissociation of the GroEL complexes during gel electrophoresis.

The relatively high stability coupled with the electrophoretic shift of GroEL caused by gp5 binding enabled the separation of the GroEL−gp5 complex from free GroEL using native agarose gels or low-percentage native polyacrylamide gels (Figures 2 and 3). Excision of the shifted and unshifted bands from the gel and analysis on an SDS−polyacrylamide gel showed that the upper band is composed of GroEL and gp5 while the lower band contains exclusively GroEL (data not shown). When [$^{35}$S]methionine-labeled gp5 was complexed with GroEL, the radioactivity was found only in the upper band (Figure 3). Upon addition of GroES and $Mg^{2+}$−ATP, the upper band decreased with time, and pentamers and hexamers of gp5 (precursors to HK97 prohead I) appeared (Figure 3). The upper band is thus a complex between refoldable gp5 and GroEL, and effective refolding of gp5 from the complex requires both $Mg^{2+}$−ATP and GroES. As shown in Figure 3, the addition of either $Mg^{2+}$−ATP or GroES alone does not affect the magnitude of the band shift. Also note that the gp5 released from GroEL is detected in the form of either hexamers or pentamers—no species that could be identified as a monomer of gp5 was found.

The radioactivity in the gel shown in Figure 3, panel A, was quantified, and the conversion of gp5 in the GroEL−gp5 complex to gp5 in pentamers and hexamers is plotted as a function of time in Figure 3, panel C. More than half of the gp5 was already in the form of 5-mers and 6-mers by 3 min after refolding initiation; within 60 min, 90% of the gp5 was refolded. Prolonged incubation of the complex with GroES and $Mg^{2+}$−ATP refolds nearly all of the gp5 in the complex (data not shown).

*Fragments of gp5 Bind to GroEL but Only the Intact gp5 (42 kDa) Reduces the Electrophoretic Mobility.* The properties of GroEL−peptide complexes derived from three fragments of gp5 were investigated. When HK97 prohead I is treated with trypsin, gp5 is cleaved into two fragments: an 18 kDa N-terminal fragment and a 24 kDa C-terminal fragment (Xie, 1994). In the transition from prohead I to prohead II, the N-terminal 11 kDa fragment is cleaved from gp5 to produce the 31 kDa processed form, gp5* (Figure 1). All three peptide fragments of gp5 interact with GroEL when renatured from GuHCl as shown from their comigration with GroEL during glycerol gradient sedimentation and size-exclusion chromatography (data not shown). On a native polyacrylamide gel, all three gp5 fragments, when renatured into GroEL, showed only a single unshifted GroEL band. When the unshifted GroEL bands were excised and run on an SDS gel, they resolved into GroEL and their respective gp5 fragments. Since all these fragments compete with gp5 in binding to GroEL (Xie, 1994), and since these peptides could be released from GroEL upon addition of GroES and $Mg^{2+}$−ATP (Table 1), we concluded that their comigration with GroEL on native gels is not simply a nonspecific binding but is involved in the same mechanism as the binding of gp5.

During native gel electrophoresis, the mobility of a protein is determined by its charge, size, and shape. Considering the size of the GroEL 14-mer (~800 kDa), and the fact that the substrate is thought to bind to the inside of the central cavity of GroEL, it seems unlikely that simply adding gp5 (42 kDa) could dramatically change the size of the GroEL complex. Thus, several interesting questions arise: What causes the lower electrophoretic mobility (band shift) of the GroEL−gp5 complex? Why does only full-length gp5 cause the band shift? It has been proposed that the N-terminal region of gp5 may promote correct assembly of gp5 subunits (Duda et al., 1995b), and it may also play a role in the refolding of gp5 from its complex with GroEL. Does the N-terminal region have a specific role in GroEL binding and in the observed band shift?

We hypothesized three possible causes of the band shift: (1) *Super-complex formation*—Two or more GroEL−gp5 complexes associate through a protruding portion of the bound gp5 monomers (the band shift is due to the larger size of the associated complexes). (2) *Conformational change*—Binding of the substrate triggers a conformational change in GroEL which in turn causes the band shift (the magnitude of the conformational change is related to the size of the bound polypeptide; a peptide that is too small will not cause a conformational change). (3) *Charge or counterion binding*—Binding of substrate polypeptide to GroEL brings more charge and/or counterions onto GroEL, and different polypeptides bring different amounts of charge. To distinguish among these possibilities, we examined what effect a series of different polypeptides have on the mobility of the GroEL complex, and whether the lower mobility

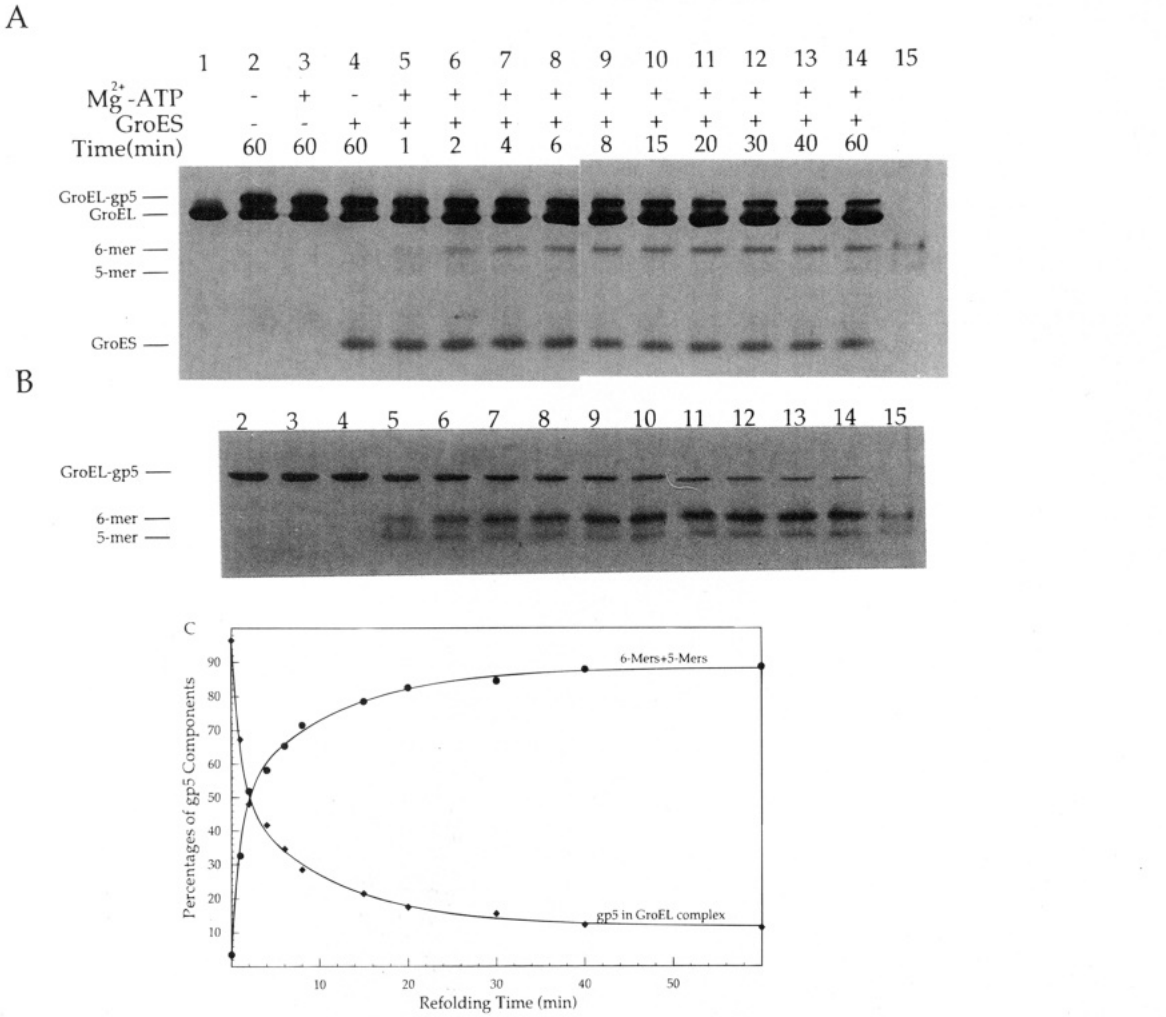


FIGURE 3: Time course of refolding of gp5 from the GroEL complex analyzed by 5% native polyacrylamide gels. The GroEL 14-mer (0.8 $\mu$M) was complexed with denatured [$^{35}$S]methionine-labeled gp5 as described under Materials and Methods. $Mg^{2+}$−ATP and GroES were added at various times to start the refolding (lanes 5−14). Final concentrations for the components are GroEL, 0.53 $\mu$M; GroES, 0.76 $\mu$M; and $Mg^{2+}$−ATP, 1.2 mM. The reaction was stopped by addition of EDTA in 4× native PAGE sample buffer. In control experiments, an equal volume of TKG was added in place of $Mg^{2+}$−ATP or GroES (lanes 2−4). The incubation time for control experiments was 60 min. Lane 1 is GroEL only. Lane 15 is 5-mers and 6-mers of HK97 prohead I made by dilution of [$^{35}$S]methionine-labeled HK97 prohead I into 10 mM Tris-HCl, pH 7.5, 1.5 M KCl, and 20% glucose (R. L. Duda and R. W. Hendrix, unpublished data). Panel A: 5% native polyacrylamide gels of the time course of refolding. Panel B: Radioautography of the gels shown in panel A. Panel C: The time course of refolding. Gels shown in panel A were scanned using an AMBIS radioanalytical imaging system. The percentages of the folded gp5 (6-mers + 5-mers) and GroEL-bound gp5 were calculated as the ratio of their respective radioactive counts to the total counts (6-mers + 5-mers + GroEL−gp5).

during native gel electrophoresis is caused by changes in size or in charge.

*Different Substrates Cause Different Band Shifts.* We formed GroEL−peptide complexes with a variety of different peptides, including a set of variants of gp5 that contain internal sequence duplications (Figure 4). All peptides formed stable complexes with GroEL as shown by their comigration with GroEL during native gel electrophoresis. Their comigration with GroEL on 5% native polyacrylamide gels was tested by excising the GroEL bands and reanalyzing them on SDS−polyacrylamide gels. The band shift of GroEL on native 5% polyacrylamide gels caused by peptide binding was measured as the distances (millimeters) from the center of the uncomplexed GroEL band to that of the complex band. All band shifts caused by substrate binding showed decreased mobility of the complexes—no complexes were found with higher mobility. The results listed in Table 1 show that different polypeptides cause different band shifts when complexed to GroEL. To relate the band shift to the properties of individual polypeptides, we calculated the mass of each substrate polypeptide, and the charge that each polypeptide is predicted to bear at pH 8.8. These values are also shown in Table 1.

The first conclusion drawn suggests that only peptides above a certain size, about 31 kDa, cause a band shift. This is a new observation, but it is in agreement with observations made by other groups; Evers et al. (1992) and Fisher (1992, 1994) reported band shifts caused by binding of peroxisomal alcohol oxidase (74 kDa) and glutamine synthetase (52 kDa) to GroEL. For polypeptides that do cause band shifts, however, the size of the substrate polypeptide apparently does not determine the magnitude of the shift. This is seen from the P22 major head protein (45 kDa) and ALDH (52 kDa); both peptides are larger than HK97 gp5, but cause smaller shifts. Though all of the HK97 gp5 mutants (except dm14) cause larger shifts than gp5, among the mutants themselves, size is not the only determinant.

The second conclusion is that the shift of the GroEL complex with an individual peptide is not directly related to the net charge that peptide is predicted to bear. On 5% native

Table 1: Different Substrates Cause Different Band Shifts[a]

| peptide name[b] | size (kDa)[c] | charge[d] | shift[e] (mm) | refolding property[f] |
|---|---|---|---|---|
| gp5 | 42.2 | −12 | 2.5 | 5-mers, 6-mers |
| $gp5_{N\text{-terminal}}$ 18 kDa | 18.6 | −4 | 0 | soluble structure |
| $gp5_{C\text{-terminal}}$ 24 kDa | 23.7 | −9 | 0 | precipitate |
| gp5* | 30.8 | −11 | 0 | precipitate |
| HK97 dm1 | 52.9 | −15 | 5.0 | smear |
| HK97 dm6 | 46.4 | −15 | 3.5 | 5-mers, 6-mers |
| HK97 dm8 | 52.4 | −13 | 3.0 | nothing |
| HK97 dm9 | 45.9 | −16 | 3.5 | 5-mers, 6-mers |
| HK97 dm11 | 49.7 | −18 | 4.5 | 5-mers, 6-mers |
| HK97 dm12 | 44.1 | −11 | 3.0 | single species |
| HK97 dm13 | 48.9 | −15 | 3.5 | single species |
| HK97 dm14 | 43.3 | −10 | 2.5 | 5-mers, 6-mers |
| HK97 dm15 | 47.5 | −11 | 3.5 | 5-mers, 6-mers |
| HK97 dm16 | 50.9 | −14 | 4.0 | 5-mers, 6-mers |
| HK97 dm17 | 51 | −21 | 6.0 | nothing |
| ALDH | 50.3 | −10 | 1.5 | |
| *Eco*RI | 30.9 | −1 | 0 | |
| Rep C | 37.7 | −3 | 0.5 | |
| P22 coat protein | 46.6 | −12 | 2.0 | |

[a] This table summarizes the properties of different GroEL−substrate peptide complexes and their interaction with GroEL. [b] The complexes formed between the peptides and 0.4 μM GroEL were analyzed on 5% native polyacrylamide gels as described under Materials and Methods. [c] The size (molecular mass) of each peptide was calculated using the GCG program "peptidesort" (Devereux et al., 1984). Each peptide was also analyzed by the GCG program "isoelectric" which plots the net charge of a peptide versus pH. [d] The charge of each peptide was measured from the plot at pH 8.0, which is the pH condition in the gel electrophoresis system. [e] The band shift caused by substrate binding was measured in millimeters as the distance between the center of the uncomplexed GroEL band to the center of the complex band. All the band shifts caused by substrate binding were exclusively because of slow mobility of the complexes. [f] The folding property (except for the N-terminal 18 kDa of gp5 which folds into a soluble structure spontaneously) is the fate of the bound substrate when $Mg^{2+}$−ATP and GroES were added to the complex and refolding was allowed to go *in vitro* as described under Materials and Methods.

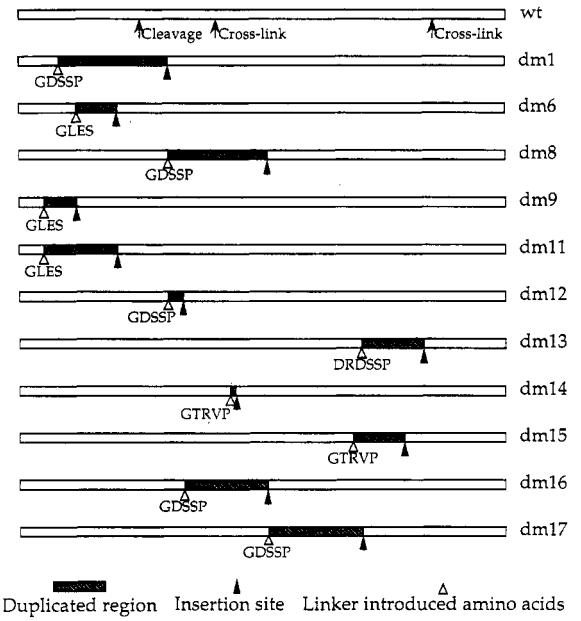


FIGURE 4: Location and length of duplication of the HK97 gene 5 duplication mutations. The duplication mutants were made from a set of linker−insertion mutants created by inserting a 12 base pair linker containing an *Xho*I site (GGACTCGAGTCC) into the gene 5 coding sequence of plasmid pT7-5Hd2.9 (Duda et al., 1995a) using the method described in Lathe et al. (1984). Plasmid DNA from each linker−insertion mutant was digested with *Xho*I and *Eco*RI. To make a duplication mutant, overlapping fragments of DNA from both plasmids, each containing the duplicated region, were ligated and transformed into BL21(DE3) cells. Ampicillin-resistant transformants were screened for the presence of a new *Xho*I site and mapped. The duplicated region in gp5 is indicated in the figure along with the linker-introduced amino acids in single-letter code. The sequence of linker-introduced amino acids varies with the restriction enzyme used to make the initial linker−insertion mutants.

polyacrylamide gels, all the proteins in Table 1 either reduce the mobility of GroEL or form a complex with no shift. Since the electrophoresis was carried out toward the anode, GroEL and all the GroEL−peptide complexes with different substrates have a negative net charge. The lower mobility of the complexes is caused by less net negative charge, by a larger size, or both. All the peptides are predicted to bear negative net charges under the conditions of electrophoresis (pH 8.8). If we were simply to add the charge of the GroEL 14-mer to that of the substrate polypeptide, we would expect more negative net charges on the complex, and the complex should have migrated faster, contrary to what we observe.

The sizes of the band shifts of the various complexes reported in Table 1 do show a reasonably good correlation with the size of the predicted net negative charge on the substrate protein. When the band shift is plotted versus the predicted net charge or the peptide size (Figure 5, panel A and panel B), a striking feature is revealed. For the peptides that cause a band shift, the magnitude of the band shift shows a good inverse correlation with the predicted negative net charge ($R^2 = 0.80$) (Figure 5, panel A). When all of the polypeptides (both those that those that do and do not cause a band shift) were included in the above analysis, the correlation is reduced ($R^2 = 0.74$). There is not as good a correlation between the band shifts and the size of the peptide ($R^2 = 0.44$ for polypeptides that cause a band shift; $R^2 = 0.69$ for all the polypeptides) (Figure 5, panel B).

*Ferguson Plot Shows That the Band Shift Is Due to a Charge Difference.* The Ferguson plot is a useful technique to distinguish between the effects of size and charge of a protein in native PAGE (Hames, 1981). In electrophoresis of a native protein, both charge and size of the protein contribute to its mobility in the gel. For a given protein, gels of different acrylamide concentration retard the protein to different degrees and change its mobility. The relative effect of charge and size on the mobility of different proteins can then be assessed by measuring the relative mobility ($R_f$) of each protein at a series of gel concentrations and plotting log $R_f$ versus gel concentration (T%), where $R_f$ is the distance migrated by the protein divided by the distance migrated by the dye. The Ferguson plot for a protein is a straight line, characterized by its slope ($K$) and its ordinate intercept. The slope ($K$) reflects the retardation of the protein by the gel, and so is directly related to the size and shape of the protein. The ordinate intercept is a measure of the mobility of the protein in free solution (T% = 0), so it is related to the net charge of the protein. Two proteins with the same size and shape but different charges will give rise to plots with the same slope but different ordinate intercepts, while protein with different sizes or shapes will show different slopes. A Ferguson plot was constructed for free GroEL and for the GroEL−gp5 complex.

Due to the large size of GroEL, the complexed and uncomplexed forms separate well only at the lower end of the range of practical acrylamide gel concentration (≤7% acrylamide); consequently, we took advantage of the excel-

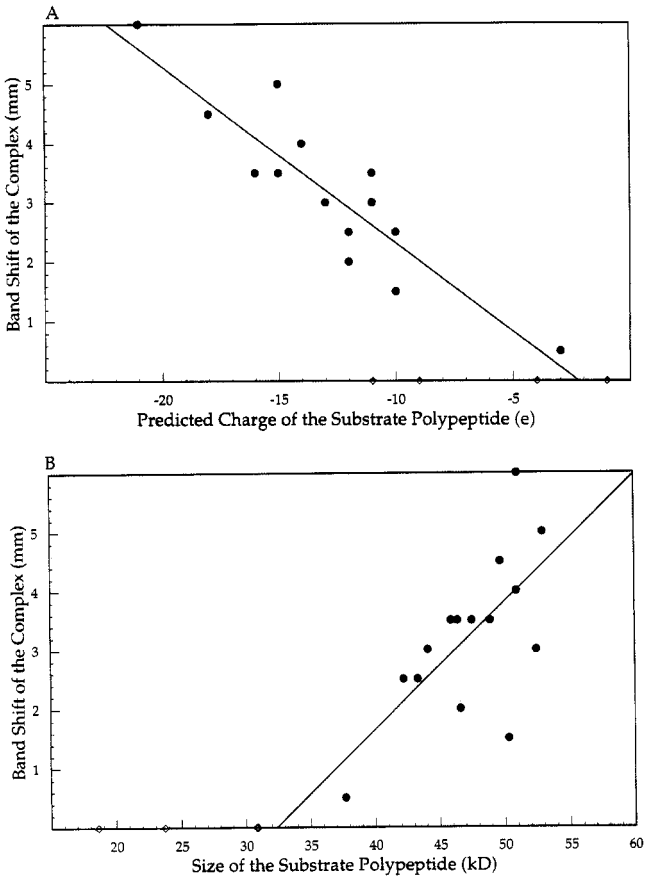


FIGURE 5: Correlation between size of the band shift and the predicted charge (panel A) and size (panel B) of the substrate polypeptide. The band shift of GroEL caused by substrate binding (as listed in Table 1) was plotted against the predicted charge and size of the substrate polypeptide, respectively. Both polypeptides that cause band shifts (solid circles) and those that do not cause a band shift (open diamonds) are included in the plots. Data from those that cause a band shift were fitted into a line. The $R^2$ for the curve-fitting in panel A is 0.80 and for Panel B is 0.44.

lent separation of the complex from free GroEL in agarose gels over a wide range of gel concentrations, and used a series of different concentration agarose gels to construct a Ferguson plot (Figure 6). The plot of GroEL parallels (same slope) that of the GroEL−gp5 complex, so different percentage gels give the same relative retardation of the two, and therefore the two have the same size. Their separation, the band shift, is therefore caused by a difference in charge. Since electrophoresis was carried out toward the anode, the GroEL−gp5 complex has less net negative charge than free GroEL. In comparison with GroEL and its complex, HK97 prohead I has a different slope and a different ordinate intercept, so the separation of HK97 prohead I from GroEL and the GroEL−gp5 complex is due to both charge and size differences. The agarose gel results are in general agreement with the limited range of observations we were able to make with polyacrylamide gels (data not shown).

*Renatured gp5 Forms a 1:1 Complex with GroEL.* Earlier *in vitro* refolding experiments show that at low GroEL concentration, maximal refolding of gp5 occurs at a 2:1 molar ratio of gp5 to GroEL (Xie, 1994). Is the band shift reported here caused by the binding of a single gp5 molecule or more than one? In an initial attempt to determine the stoichiometry of GroEL and gp5 in the complex, we measured the relative amounts of the two proteins in the GroEL−gp5 complex band resolved by native PAGE. [$^{35}$S]methionine-labeled

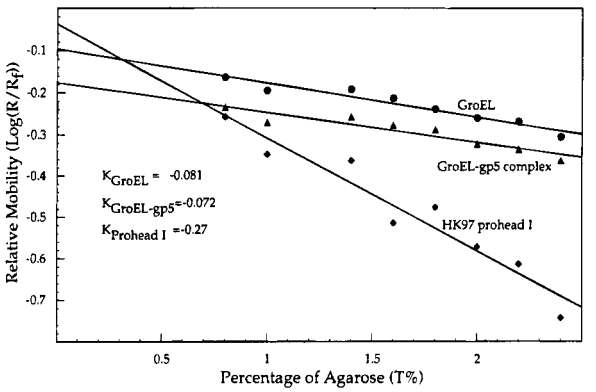


FIGURE 6: Ferguson plot shows that the GroEL band shift caused by gp5 binding is due to a charge difference. The relative mobility ($R_f$ = distance migrated by protein/distance migrated by dye) of HK97 prohead I, GroEL, and the GroEL−gp5 complex in gels of different percentage of agarose was measured as described under Materials and Methods. The logarithm of relative mobility was plotted against agarose gel percentage (T%). The slope ($K$) for each protein reflects the retardation of the protein by the gel, so it is directly related to the size of the protein. The plot of GroEL parallels that of the GroEL−gp5 complex, so agarose gels of different agarose percentage have the same retardation on both GroEL and the GroEL−gp5 complex, implying that uncomplexd GroEL has about the same size as the GroEL−gp5 complex. The different intercepts of GroEL and the GroEL−gp5 complex imply that the band shift caused by gp5 binding is due to a charge difference. The HK97 prohead I, which has different charge and size compared to GroEL, has a different slope on the plot.

GroEL was complexed with [$^{35}$S]methionine-labeled gp5. The complex was separated from unbound GroEL by a 5% native PAGE. The gp5−GroEL complex band was excised, and the protein was electroeluted. The eluted protein was analyzed by SDS−PAGE along with a series of standard mixtures. The standard mixtures contained equal amounts of [$^{35}$S]methionine-labeled GroEL protein, but different amounts of [$^{35}$S]methionine-labeled gp5, with the molar ratio of GroEL 14-mer to gp5 monomer ranging from 1.5 to 0.4. The concentrations of GroEL and gp5 were determined by quantitative amino acid composition analysis before they were mixed together. The SDS gels were scanned on a densitometer for Coomassie brilliant blue binding and on an Ambis radioimager for radioactivity. The ratio of GroEL to gp5 in the eluted protein was compared with the standard mixtures. A molar ratio of 1.3 (gp5 monomer to GroEL 14-mer) was given by both methods. This suggests that one GroEL 14-mer can bind at least one gp5 monomer.

To eliminate the ambiguity in the stoichiometry, we exploited several mutant forms of gp5 that cause different band shifts on native polyacrylamide gels (Figure 4 and Table 1). One of the mutant proteins, dm11, which has a 68 amino acid duplication close to the N-terminus of gp5, causes a slightly larger shift than wild-type gp5 (Figure 7, lanes 2 and 3). When premixed, denatured wild-type gp5 and dm11 were complexed with GroEL, they formed two well-resolved complex bands with the mobilities of the bands formed by complexes of the individual proteins. There is no band of intermediate mobility as would have been expected if GroEL could form a complex with two substrates (Figure 7, lanes 4 and 5). Thus, one GroEL 14-mer can apparently bind only one wild-type gp5 polypeptide or only one dm11 polypeptide, but not both. The duplication at the N-terminal region does not make dm11 a completely different peptide with respect to GroEL interaction and folding because upon addition of GroES and $Mg^{2+}$−ATP, dm11 can be released from the

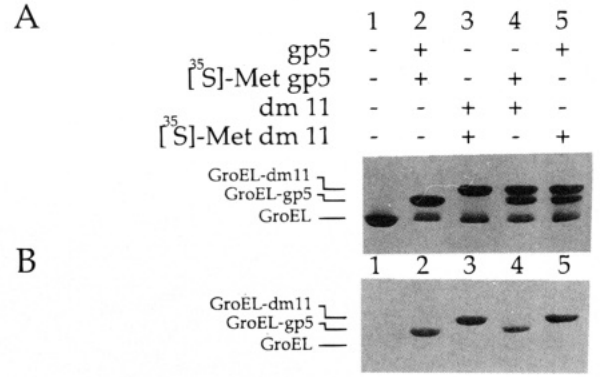


FIGURE 7: Partially renatured gp5 forms a 1:1 binary complex with GroEL. The protein product of HK97 gene 5 internal duplication mutation, dm11, causes a slightly greater band shift than wild-type gp5, when it binds to GroEL. This difference was exploited to show that GroEL forms a 1:1 complex with HK97 head protein. Lane 1, GroEL; lane 2, GroEL−gp5 complex; lane 3, GroEL−dm11 complex; lane 4, GuHCl-denatured [$^{35}$S]methionine-labeled gp5 was mixed with denatured dm11 first, and the mixture was allowed to complex with GroEL; lane 5, similar to lane 4, except that complex was formed with gp5 and [$^{35}$S]methionine-labeled dm11. In lanes 4 and 5, gp5 and dm11 do not comigrate with each other in their complexes with GroEL, showing that one GroEL 14-mer can bind only one HK97 head protein polypeptide. Panel A: A 5% native polyacrylamide gel. Panel B: Radioautograph of the gel shown in panel A.

GroEL complex into native-like 5-mers and 6-mers. It also can form hetero-5-mers and hetero-6-mers with wild-type gp5 when they are refolded together (data not shown). These results argue that GroEL cannot bind more than one gp5 at the same time. The stoichiometry is strictly 1:1.

*The GroEL−gp5 Complex Is in Dissociation/Reassociation Equilibrium in the Absence of GroES and $Mg^{2+}$−ATP.* Using a mutant GroEL, Weissman et al. (1994) showed that in the presence of $Mg^{2+}$−ATP, rhodanese bound to GroEL undergoes multiple rounds of binding and release of non-native forms even in the absence of GroES. A similar result was obtained for RuBisCO bound to GroEL (Todd et al., 1994). We used the band shift discussed here to test whether bound gp5 can be released from one GroEL 14-mer and rebound to a different one. If gp5 can be exchanged among different GroEL's, then adding [$^{35}$S]methionine-labeled GroEL to a preformed complex of gp5 and nonradioactive GroEL would enable us to see the [$^{35}$S]methionine-labeled GroEL converted from the lower band to the upper band as the gp5 exchanges from the nonradioactive to the radioactive GroEL.

In Figure 8, a complex was formed using unlabeled GroEL and unlabeled gp5 (lane 3). A mixture of unlabeled GroEL and [$^{35}$S]methionine-labeled GroEL was added to the complex (lane 4). From the radioautography, we can see that some of the [$^{35}$S]methionine-labeled GroEL was converted to the upper band. Thus, GroEL added later is still able to form a complex. When unlabeled GroEL was added first to complex any excess gp5, added [$^{35}$S]methionine-labeled GroEL was still converted into the upper band (lane 5). When gp5 was renatured into buffer without GroEL, it lost the ability to form a complex with GroEL added later (lane 2). The conversion of [$^{35}$S]methionine-labeled GroEL into complex form must be a result of dissociation of gp5 from a preformed complex.

To eliminate the effects of possible trace amounts of contaminating GroES and $Mg^{2+}$−ATP (which we regarded as very unlikely judging by the purity of GroEL and its

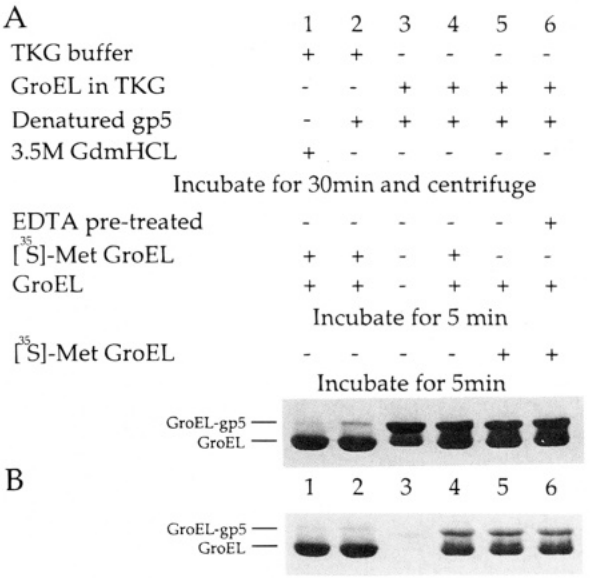


FIGURE 8: GroEL−gp5 complex is in dissociation/reassociation equilibrium even in the absence of GroES and $Mg^{2+}$−ATP. Preformed GroEL−gp5 complexes were made under standard conditions and then mixed with additional labeled and unlabeled GroEL to monitor the exchange of gp5 between complexed GroEL with the free GroEL. Samples were analyzed on a 5% native polyacrylamide gel after incubations as described below. In lanes 3−6, the starting material was 0.8 $\mu$M GroEL−gp5 complex. Lane 3 shows the GroEL−gp5 complex without any treatment. In lane 4, 30 $\mu$L of GroEL−gp5 complex was mixed with 5 $\mu$L of 2.4 $\mu$M unlabeled GroEL and 5 $\mu$L of 2.4 $\mu$M [$^{35}$S]methionine-labeled GroEL, and incubated for 10 min. In lane 5, unlabeled GroEL was added and incubated for 5 min before [$^{35}$S]methionine-labeled GroEL was added. Lane 6 is similar to lane 5 except that the GroEL−gp5 complex, unlabeled GroEL, and [$^{35}$S]methionine-labeled GroEL were all pretreated with EDTA. Lane 1 shows uncomplexed GroEL treated under the conditions described with no gp5. For lane 2, denatured gp5 was first diluted into TKG, and GroEL (to 0.8 $\mu$M) was added later. See Materials and Methods for additional details. Panel A: A 5% native polyacrylamide gel. Panel B: Autoradiograph of the gel shown in panel A.

method of purification), both the GroEL−gp5 complex and the added GroEL were pretreated with EDTA. EDTA has no effect on the conversion of [$^{35}$S]methionine-labeled GroEL with GroEL in the preformed complex (lane 6). The gel shown in Figure 8, panel A, was scanned by a densitometer and analyzed on an AMBIS radioanalytical imaging system. The former measured the amount of protein in the upper band (GroEL and gp5) and in the lower band (GroEL only). The latter measured the amount of [$^{35}$S]methionine-labeled GroEL in both the upper and lower bands. The percentage of protein (total protein by densitometer and [$^{35}$S]methionine-labeled GroEL by radioactivity) in the upper band relative to the sum of the upper band and the lower band was calculated. The result is shown in Table 2. Both methods give consistent results regarding the redistribution of GroEL in the GroEL−gp5 complex solutions. The higher percentage measured by the densitometer is probably because it measures both GroEL and gp5 for the upper band; since GroEL has no tryptophan, it may have different Coomassie brilliant blue binding properties. It should be noted that the same ratios were obtained when the labeling pattern was reversed.

Because there is 0.17 M GuHCl in the GroEL−gp5 solution (as a result of the 20-fold dilution of the gp5 solution containing 3.5 M GuHCl), we asked whether the equilibrium between GroEL-bound and free gp5 might be perturbed by

Table 2: Equilibrium Binding and Releasing of gp5 from the GroEL−gp5 Complex[a]

| | lane no. | | | | | |
|---|---|---|---|---|---|---|
| | 1 | 2 | 3 | 4 | 5 | 6 |
| % by densitometer | | | 91.7 | 41.6 | 40.9 | 39.9 |
| % by radioactivity | 5.0 | 4.5 | | 27.0 | 26.2 | 25.1 |

[a] The gel shown in Figure 8 was scanned by a densitometer before it was dried for radioactivity measurement on an AMBIS radioanalytical imaging system. The percentage of protein listed was calculated as: the upper band signal/(the upper band signal + the lower band signal). [Note: The densitometer measurement was done using a single gel. The radioactivity measurement was done using two identical gels, and the results were averaged.]

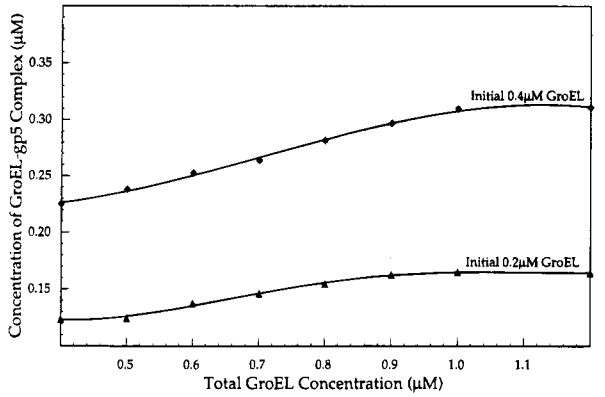


FIGURE 9: Measurement of total gp5 present in the GroEL−gp5 complex solution. [$^{35}$S]methionine-labeled GroEL (0.2 $\mu$M) was mixed with denatured gp5 to form GroEL−gp5 complexes, as described under Materials and Methods. To bring any remaining unbound gp5 in the reaction mix into complexed form, equal volumes of different concentrations of [$^{35}$S]methionine-labeled GroEL were mixed with the initial GroEL−gp5 complex solution. After 30 min of equilibration, samples were run in a native gel to separate the complex and the free GroEL. The dried gel was scanned on an AMBIS radioanalytical imaging system to obtain the upper and lower band counts. The concentration of the GroEL−gp5 complex was calculated as [final GroEL concentration] × [upper band counts/(upper band counts + lower band counts)]. The experiment was repeated with an initial concentration of 0.4 $\mu$M [$^{35}$S]methionine-labeled GroEL−gp5 complex. The results were plotted versus final GroEL concentration (the free GroEL + the complexed GroEL) in the experiment.

0.17 M GuHCl. We therefore repeated the experiment in such a way that the final GuHCl concentration was 0.06 M, and the equilibrium did not appear to be affected (data not shown). We conclude that the equilibrium is not dramatically perturbed by the amount of GuHCl present in our experimental system. The GroEL−gp5 complex is in equilibrium with free GroEL and free incompletely folded gp5 even without the action of GroES and ATP.

If the above conclusion is true, then more free GroEL added to the complex solution should disturb the equilibrium and more free gp5 should be converted into the GroEL-bound form. As shown in Figure 9, when increasing amounts of GroEL are added, the amount of gp5 captured in the complex increases until all the gp5 is found in the complex form. At an initial GroEL concentration of 0.40 $\mu$M, the total [gp5] (both GroEL-bound and free gp5) was 0.46 $\mu$M. At an initial GroEL concentration of 0.20 $\mu$M, the total [gp5] is 0.25 $\mu$M. Thus, though the binding stoichiometry of GroEL to gp5 is 1:1, at equilibrium there is more gp5 in the solution than GroEL can possibly bind. The estimated dissociation constant based on data presented in Figure 9 is on the order of $10^{-7}$ M. (See Materials and Methods for the method of calculation.)

*Trypsin Digestion of the gp5−GroEL Complex Eliminates the Band Shift by Gradually Removing the N-Terminus of gp5.* Since the 42 kDa gp5 induces a significant band shift while the 31 kDa gp5* causes no shift at all, we examined the possibility that intermediate-sized fragments of gp5 could cause a band shift. The fact that rhodanese bound to GroEL is accessible to trypsin digestion suggests that substrates are at least partly accessible when bound to GroEL. It also suggests that trypsin digestion of the GroEL−gp5 complex may give some clue as to what causes the band shift. We treated the GroEL−gp5 complex with trypsin for different times, stopped the reaction with PMSF, TLCK, and STI (soybean trypsin inhibitor), and analyzed the products by both native and SDS−polyacrylamide gels (Figure 10).

The native polyacrylamide gel (Figure 10, panels A and B) displaying the time course of digestion shows that the (shifted) upper band progressively moved down to the GroEL position as digestion proceeded. Comparison with an SDS gel of the same samples (Figure 10, panels C and D) shows that the disappearance (over time) of the upper band in the native gel corresponds to the disappearance of gp5 in the SDS gel. From the autoradiography of the native gel, we see that trypsin digestion produces one distinct intermediate shifted band (right above the free GroEL band); this intermediate band is probably related to the 36 kDa fragment seen in the SDS gel. This result argues that there is an intermediate-sized gp5 fragment that can cause an intermediate band shift (Figure 10, panels C and D, band 1). The 33−31 kDa fragments cause no band shift, as shown in lanes 8 and 9 in Figure 10, panels A and B.

Note in Figure 10 (panels C and D), trypsin digestion of the gp5−GroEL complex produces four major fragments from gp5 (band 1−band 4); one is 36 kDa, and the other three are smaller (31 kDa, 32 kDa, and 33 kDa). At later times, the 36 kDa fragment was further digested while the three 31−33 kDa fragments seemed relatively stable (Figure 10, panel E). The SDS gel with trypsin digestion of the GroEL−gp5 complex was electroblotted for N-terminal sequencing; the results for the four new bands are listed in Figure 11. From Figure 11, we see that the four bands were produced by a series of cleavage sites in the N-terminal region of gp5. Band 4 shown in Figure 10 is actually two fragments of gp5. One has the same N-terminus as the 31 kDa gp5* in HK97 prohead II. The five fragments emerge roughly simultaneously; all five tryptic cutting sites probably have a similar accessibility to trypsin. The 36 kDa fragment (band 1 in Figure 10, panels C and D) was later converted mainly into 33−31 kDa fragments (band 2−band 4). It appears the 33 and 32 kDa fragments were later converted into the 31 kDa fragments, which seem more resistant to tryptic digestion. Prolonged digestion of gp5 bound to GroEL gave a digestion pattern below 31 kDa similar to that of the digestion of gp5*-bound GroEL under the same conditions (data not shown).

The gel shown in Figure 10, panel C, was scanned and analyzed on an AMBIS radioanalytical imaging system to determine the radioactivity of gp5 and that of the 36 kDa fragment for each lane. Since the 31, 32, and 33 kDa fragments are too close to each other to be resolved in the AMBIS, we measured the sum of their counts. The counts for the fragments were scaled by their methionine residue numbers relative to that of gp5 and normalized against the

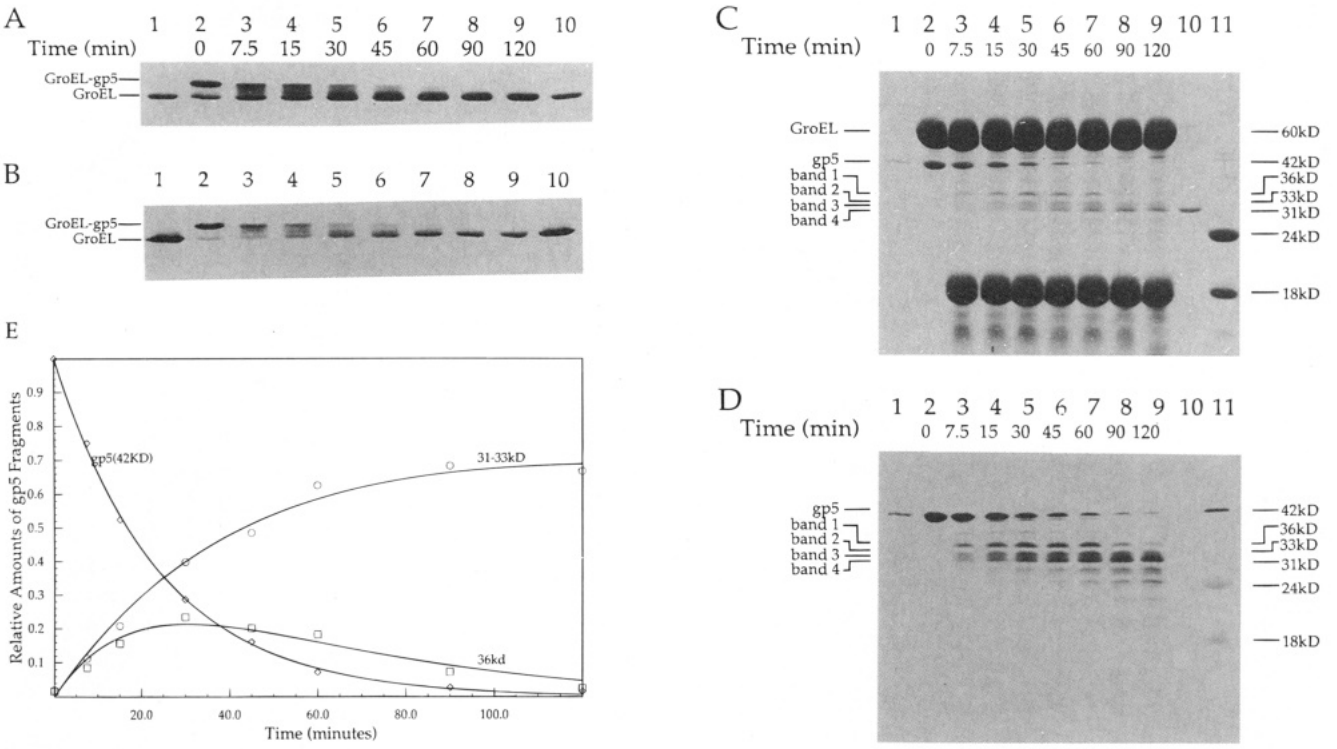


FIGURE 10: Time course of trypsin digestion of gp5 bound to GroEL. GroEL 14-mer solution (0.26 $\mu$M) was complexed with [$^{35}$S]-methionine-labeled gp5 as described. Digestion was initiated by addition and quick-mixing of 10 $\mu$g/mL trypsin to the complex at various times so that the digestion times were 7.5, 15, 30, 45, 60, 90, and 120 min. To stop the digestion, PMSF, STI, and TLCK were added. A portion of each sample was analyzed by a 5% native polyacrylamide gel; the rest of each sample was precipitated with TCA and analyzed on a 12.5% SDS−polyacrylamide gel. Panel A: A 5% native polyacrylamide gel. Lanes 1 and 10, [$^{35}$S]methionine-labeled GroEL only; lane 2, GroEL−[$^{35}$S]methionine-labeled gp5 complex; lanes 3−9, time course of digestion at 7.5, 15, 30, 45, 60, 90, and 120 min. Panel B: Radioautograph of panel A. Panel C: A 12.5% SDS gel. Lane 1, gp5 only; lane 2, GroEL−gp5 complex; lanes 3−9, time course of digestion at 7.5, 15, 30, 45, 60, 90, and 120 min; lane 10, gp5*(31 kDa); lane 11, N-terminal 18 kDa and C-terminal 24 kDa fragments of gp5 from trypsin digestion of HK97 prohead I. The heavy bands at about the 18 kDa position in lanes 3−9 were from STI and trypsin. Panel D: Radioautography of panel C. Lane 11 in panel C was made by mixing trypsin-digested HK97 prohead I with [$^{35}$S]methionine-labeled undigested prohead I when preparing for the SDS gel samples, so the [$^{35}$S]methionine-labeled gp5 has not been completely digested as shown on the radioautography. Panel E: Time course of trypsin digestion as measured by the disappearance of gp5 and the appearance of some of the digestion fragments. The gel shown in panel C was scanned and analyzed on an AMBIS radioanalytical imaging system. The radioactive counts in gp5 and in the 36 kDa fragment were measured for each lane. Since the 31, 32, and 33 kDa fragments are too close to each other to be resolved in the AMBIS system, we measured the sum of their counts. The counts for the 36 and 31−33 kDa fragments were scaled according to their methionine content relative to that of gp5. All the counts were normalized against the gp5 count at $t = 0$ (panel C, lane 2).

gp5 count at $t = 0$. The result is plotted as a function of time in Figure 10 (panel E). The data fit with a simplified model predicting that cleavage occurs at a substantial but equal rate at sites that lead to a 36 kDa fragment and 31−33 kDa fragments from gp5, and to 31−33 kDa fragments from a 36 kDa fragment (the sites labeled 1 through 4 in Figure 11, about 0.019/s). Cleavage also occurs at much lower rates on other sites that lead to the production of fragments smaller than 31 kDa (0.0036/s for gp5, 0.007/s for 36 kDa, and 0.001/s for 31−33 kDa). Thus, trypsin digestion reveals that the N-terminus of gp5 bound to GroEL is much more accessible to trypsin digestion than the C-terminus and is therefore likely to be less compact (or more flexible). Further, the data give evidence for a complex with an intermediate band shift that correlates with the presence of an intermediate sized (36 kDa) protein.

## DISCUSSION

*Conformation of gp5 Bound to GroEL.* In this paper, we describe the formation of a stable complex between gp5 and GroEL and the properties of that complex as revealed by a gel electrophoresis study. Studies of other peptides bound to GroEL suggest that they are in a "molten globule"-like intermediate conformation (Martin et al., 1991). A molten globule lacks tertiary structure but contains a significant amount of secondary structure (Landry et al., 1994; Zahn et al., 1994), as suggested by NMR (Flynn et al., 1993; Zahn et al., 1994), tryptophan fluorescence, protease digestion, and hydrophobic dye binding experiments (Martin et al., 1991; Mendoza et al., 1992). Direct interaction of folding intermediates with GroEL has also been interpreted to suggest molten globule-like properties (Hayer-Hartl et al., 1994). Tryptophan fluorescence of gp5 bound to GroEL indicates that the five Trp residues in gp5 are exposed to a hydrophobic environment (Xie, 1994). Trypsin digestion of the gp5 bound to GroEL as described above shows that the GroEL-bound gp5 is flexible with many tryptic cleavage sites exposed. Thus, the GroEL-bound gp5, like other GroEL substrates, appears to be molten globule-like when bound to GroEL.

A striking contrast is seen in the N-terminal region of gp5 because this section of the GroEL-bound protein appears more accessible to trypsin than the C-terminus. There are two possible explanations for this. The first is that, as will be discussed later, the central cavity of the GroEL 14-mer is not large enough to hold the entire gp5, so part of the N-terminus might protrude from the complex. The second possibility is that the tryptic cleavage actually occurs in the medium after gp5 has been released from GroEL; in this

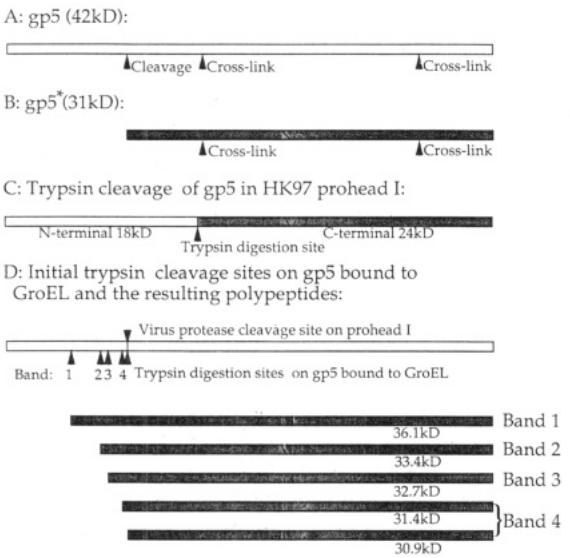


FIGURE 11: Protease cleavage sites and some of the resulting peptides of gp5. (A) gp5, the 42 kDa head protein of HK97 prohead I with viral protease cleavage site (K103), and subsequent cross-liking sites (K169 and N356) are shown (Duda et al., 1995a,b). (B) The 31 kDa peptide, gp5*, is the cleaved form of gp5 in HK97 prohead II. (C) Trypsin digestion of gp5 in HK97 prohead I produces two fragments, the N-terminal 18 kDa and the C-terminal 24 kDa (Xie, 1994). (D) Some of the initial trypsin cleavage sites found on gp5 bound to GroEL. The N-terminal sequences were determined for the peptides in bands 1 through 4 in the gel shown in Figure 10, panel C. Trypsin cleavage sites and corresponding peptides are shown for bands 1−4. Band 1 is the result of cleavage at R55, band 2 is from cleavage at R80, and band 3 is from K87. Band 4 is a a mixture of two bands reulting from K99 and K103. Note that K103 is also the viral protease cleavage site.

model, the N-terminus is more accessible to trypsin because it is much more flexible than the C-terminus. Several experimental results seem to support the second explanation. The N-terminal 18 kDa fragment produced by tryptic digestion of HK97 prohead I has GroEL binding ability. The complex formed between gp5* and GroEL undergoes dynamic dissociation and reassociation as shown above for the GroEL−gp5 complex (data not shown). Trypsin digestion of gp5* complexed to GroEL reveals that the time scale and the digestion pattern on the SDS gel in the region below 31 kDa are similar to those of trypsin digestion of gp5 bound to GroEL (data not shown).

*Quasi-Equilibrium Process of Dissociation/Reassociation of the GroEL−gp5 Complex.* The GroEL−gp5 complex is stable at room temperature; 24 h after formation of the complex, most of the gp5 can still be refolded into functional 5-mers and 6-mers upon addition of GroES and $Mg^{2+}$−ATP. However, the gp5 will aggregate upon further storage of the complex. Previous experiments show that unfolded gp5 aggregates rapidly when diluted into buffer in the absence of GroEL. Subsequent addition of GroEL does not rescue the protein from self-aggregation (Xie, 1994; Figure 8).

These results suggest the GroEL-mediated refolding of gp5 can be described as a two-phase process: a fast initial phase followed by a quasi-equilibrium phase. The initial phase occurs very rapidly as soon as gp5 is diluted into GroEL whereupon it folds into intermediate structures (molten globule-like compact structures with exposed hydrophobic surfaces). Because of the exposed hydrophobic surfaces, these gp5 intermediates tend to either aggregate with each other or bind to GroEL. The latter, of course, shields the intermediates from aggregation. A quasi-equilibrium is achieved by the end of the initial phase, with the complex dissociating and reassociating. However, gp5 that is released into the medium can still irreversibly self-aggregate so that it is not a true equilibrium.

Our result that GroEL-bound gp5 undergoes a dynamic dissociation/reassociation process is consistent with reported experimental results on other proteins. RuBisCO bound to GroEL could be released into solution in the absence of ATP and GroES in a non-native form and rebound to a different GroEL molecule (Todd et al., 1994). Similarly, rhodanese and ornithine transcarbamylase (OTC) bound to GroEL could be released into a non-native form in the presence of $Mg^{2+}$−ATP (Weissman et al., 1994). This dynamic dissociation/reassociation of the GroEL−substrate complex may well be a general property of chaperonins (Weissman et al., 1994).

Dissociation constants of GroEL−substrate complexes are difficult to measure because of their intrinsic nature. Todd et al. (1994) used a competition method to estimate a value of 120 min for the dissociation rate of a RuBisCO−GroEL complex; assuming that the association is diffusion-limited, these authors reported an estimate of 1 pM for the dissociation constant of this complex. This contrasts sharply with the value of 100 nM we obtained from the ratio of free and gp5-bound GroEL on our native polyacrylamide gels. Of course, both the substrates and the conditions of the experiments were different; both are expected to influence the value of the dissociation constant. The gel itself would also perturb the equilibrium. However, it seems unlikely that we would observe any free GroEL under the conditions of our experiments, including gp5 excess, if the dissociation constant were on the order of 1 pM. We therefore conclude that 100 nM is a better estimate of the gp5−GroEL dissociation constant (under our conditions). This raises interesting questions requiring further experimental work. Perhaps the GroEL−substrate dissociation constant is highly variable, depending on the substrate and on the conditions. If so, that would be important to its function. An alternative possibility (that is not mutually exclusive) is that the association/dissociation kinetics are more complicated than assumed by Todd et al. That would also be important to its function, but more data would be needed to distinguish these possibilities.

*The Origin of the Band Shift and Its Implication for the Interaction between GroEL and Its Substrates.* It has been suggested that the partially folded peptide, presumably in a molten globule-like structure, binds to the central cavity of GroEL through hydrophobic interactions. Cryo-electron microscopic images of both free GroEL and the GroEL−malate dehydrogenase (34 kDa) complex were reported by Chen et al. (1994), who concluded that the substrate fills one end of the central cavity of GroEL with a density similar to that of its native structure, leaving some material protruding slightly from the end. Similarly, Weissman et al. (1994) used the crystal structure of free GroEL (Braig et al., 1994) to suggest that a medium-size substrate such as rhodanese (33 kDa) is barely able to fit within GroEL's central cavity, even if the substrate were in the highly compact native state. Both lines of evidence suggest there is an upper limit to the size of substrate that can be accommodated in the central cavity of GroEL. For larger substrates, Weissman et al. (1994) suggested the central cavity would need to undergo a radical increase in diameter. Our experiments show that only peptides above a certain minimum size (approximately 31−33 kDa) can cause the band shift of GroEL during native

gel electrophoresis. The minimum size needed to promote the band shift is about 30−31 kDa from the data presented, but this value may change when more proteins have been tested. The total number of charged residues and the net charge of gp5 are fairly evenly distributed in its sequence [see Duda et al. (1995a,b)], suggesting that a grossly unusual charge distribution is not required to produce the band shift. We found that three separate fragments of gp5, which encompass the entire sequence of gp5, bind to GroEL without causing a band shift. The fact that none of these parts (the C-terminal 31 kDa gp5*, the N-terminal 18 kDa, and the C-terminal 24 kDa; Figure 11 and Table 1) causes a band shift, while the whole gp5 does, implies that it is the size of the peptide and not any specific sequence that determines whether the band shift occurs. It is probably not coincidental that the minimum size of peptide that can cause a band shift can be related to the size of the central cavity of GroEL. We therefore suggest this electrophoretic band shift is associated with a change in the complex consequent to a complete filling of the central cavity.

However, the Ferguson plots suggest that the gp5-associated band shift is due primarily to a lower negative net charge on the GroEL−gp5 complex. In Figure 6, we presented the Ferguson plots of GroEL and the GroEL−gp5 complex. Similar results have also been obtained for the GroEL−dm1 complex and the GroEL−dm11 complex, strengthening the argument that the band shift is due to a charge difference. How is a filling of the central cavity connected to an apparent charge difference?

These observations raise another apparent paradox. All the band shifts we have observed (see Table 1) represent a reduction of the electrophoretic mobility of the corresponding complexes. Given the direction of the electric field, this corresponds to complexes with less negative charge than free GroEL. However, all of the substrates are predicted to bear negative net charge at the pH of the experiment. The use of the simple prediction method, which is based on p$K_a$'s of the constituent amino acid side chains, seems reasonable for a molten globule-like substrate. Free GroEL 14-mers also carry a negative charge; *i.e.*, the complex should be slightly more negatively charged than free GroEL, not less. This is compounded by the observation of a significant correlation between the magnitude of the band shift and the absolute value of the charge on the substrate (Figure 5). The correlation is not unreasonable, but the sign is in the wrong direction.

What is the source of the incremental positive charge responsible for the altered electrophoretic mobility? Two possible sources of additional positive charges are protons or cations present in the solutions used in our experiments. A series of band shift experiments in agarose gels, conducted over a range of experimental pH (6.5−8.5), showed that there was no significant change in the magnitude of the band shift (data not shown). These results argue that the band shift is not a result of proton uptake by the complex. We therefore suggest the band shift results from uptake by the complex of cations, *e.g.*, $K^+$, which were present in the solutions used in our experiments. This hypothesis raises several questions, including the following: Where could the cations be bound? Why does this occur only when the substrate is larger than 31 kDa? Does this account for the variable magnitude of the band shift seen in our results?

Each GroEL subunit is predicted to contain 20 net negative charges at the pH of our experiments. This corresponds to a total of −280 eu for the entire 14-mer. Contrasting this, the predicted charge on the substrate protein is −10 to −20 eu. Clearly, the charge on the GroEL molecule itself dominates. We therefore first consider the possible uptake of cations there.

Movement(s) of domains, particularly the apical domains, is (are) one likely mechanism of conformational change in the gp5−GroEL complex. Another is the ordering of regions that were disordered in the unliganded protein (Braig et al., 1994). Either could bring negatively charged surfaces into close proximity, leading to, if not requiring, the binding of positively charged counterions. In principle, this could "explain" a reduced mobility for the complex. Could it explain a variable magnitude for the band shift? Given that there are 14 subunits in the GroEL complex, there could be as many as 15 states of the 14-mer even with only 2 conformational states for each subunit. With more than two states, the combinatorial possibilities become much larger. If the microstates involve different numbers of bound cations, then a potentially large number of different values for the net charge of the complex is possible. Another potential source of variability is described below.

These observations may be related to those of Horowitz et al. (1995), who showed that the hydrophobic surface area of the native GroEL molecule is restricted. They also reported that ionic interactions, especially those with cations, are effective in increasing the hydrophobic surface area (Horowitz et al., 1995). The crystal structure of GroEL reveals the main areas of flexibility are in the apical domain between residues 220 and 360 (Braig et al., 1994). Fenton et al. (1994) introduced site-specific mutations, showing that hydrophobic residues in the apical domain are involved in the binding of substrate and GroES.

Another potential site for cation binding comes from a curious feature of the current model of peptide−GroEL interaction. The generally accepted view has the substrate binding to the inner surface of the GroEL toroid by largely hydrophobic interactions, *i.e.*, with the substrate lining the inner cavity of GroEL. That would seem to require the substrate protein to be turned topologically inside-out from the usual "oil drop" model, in order to place its hydrophobic residues against the wall of the inner cavity of GroEL. This may not be a problem for a small substrate, but as the size of the substrate approaches that of the GroEL cavity things could get rather crowded. Where do the charged residues end up? Given that the average radius of the cavity (in the unliganded protein) is about 23 Å (Braig et al., 1994), many of them could end up near the central axis of the cylinder. For a negatively charged substrate, such as gp5, it could force some negative charges into close proximity, requiring more counterions. While this could account for (some of) the variability of the band shift, it would seem unlikely that cations would be bound in excess of the net charge on the substrate, *i.e.*, the sign paradox described above.

The results reported here are consistent with previous reports that the GroEL−substrate complex is more stable at higher salt concentration and lower temperature. Those observations are characteristic of a hydrophobic interaction, but we now see that there may be an additional electrostatic component of the interaction. Our data seem to require the binding of cations, probably at negative charges that are being brought into proximity somehow by binding of substrate to GroEL. These ions may not be specific although it is one potential explanation for the $K^+$ requirement. Pretreatment

of all solutions (denatured gp5, GroEL, and electrophoresis buffers) with chelators (EDTA, EGTA, and OP) did not eliminate the band shift, although the affinity of the complex was reduced (data not shown).

The involvement of both electrostatic interactions and hydrophobic interactions has been proposed for other chaperonins. SecB binds both positively charged peptides and the hydrophobic fluorescent probe 1,8-ANS (Randall, 1992). Randall also proposed that SecB interacts with substrates by binding to positively charged regions on the substrate; this induces a conformational change in SecB leading to additional binding (Randall, 1992). Similarly, it has been suggested that DnaK interacts with bound peptide through substrate backbone hydrogen bonds as well as hydrophobic interactions and salt-bridges (Landry et al., 1992). Thus, not surprisingly, chaperonin−substrate interactions probably involve all the forces known to be important in maintaining protein stability.

*Model of the GroEL-Facilitated Refolding System.* Binding of partly folded proteins to GroEL has two functions; one is to prevent the aggregation of folding intermediates by binding and sequestering them. This is the original role that suggested the name "chaperonin" because they prevented "illicit associations". More recent suggestions by Lorimer, Horwich, and their respective co-workers (Todd et al., 1994, Weissman et al., 1994) invoke a more active role in which the energy liberated by ATP hydrolysis is used to unfold misfolded intermediates or kinetically trapped (off-pathway) states, perhaps releasing them into one or more pathways where efficient folding is possible. Our experimental results are consistent with both models of the function of GroEL.

## ACKNOWLEDGMENT

We thank Craig Peebles, James Franzen, Graham Hatfull, and Kathleen Martincic for useful discussions and Kathleen Martincic for constructing the dm mutants.

## REFERENCES

Anfinsen, C. B. (1973) *Science 181*, 223−230.
Braig, K., Simon, M., Furuya, F., Hainfeld, J. F., & Horwich, A. L. (1993) *Proc. Natl. Acad. Sci. U.S.A. 90*, 3978−3982.
Braig, K., Otwinowski, Z., Hegde, R., Biosvert, D. C., Joachimiak, A., Horwich, A. L. and Sigler, P. B. (1994) *Nature 371*, 578−586.
Chandrasekhar, G. N., Tilly, K., Woolford, C., Hendrix, R., & Georgopoulos, C. (1986) *J. Biol. Chem. 261*, 12414−12419.
Chen, S., Roseman, A. M., Hunter, A. S., Wood, S. P., Burtson, S. G., Ranson, N. R., Clarke, A. R., & Saibil, H. R. (1994) *Nature 371*, 261−264.
Dessauer, C. W., & Bartlett, S. G. (1994) *J. Biol. Chem. 269*, 19766−19776.
Devereux, J., Haeberli, P., & Smithies, O. (1984) *Nucleic Acids Res. 12*(1), 387−395.
Duda, R. L., Hempel, J., Michel, H., Shabanowitz, J., Hunt, D., & Hendrix, R. W. (1995a) *J. Mol. Biol. 247*, 618−635.
Duda, R. L., Martincic, K., & Hendrix, R. W. (1995b) *J. Mol. Biol. 247*, 636−647.
Earnshaw, W., Casjens, S., & Harrison, S. (1976) *J. Mol. Biol. 104*, 387−410.
Ellis, R. J., & van der Vies, S. M. (1991) *Annu. Rev. Biochem. 60*, 321−347.
Evers, M. E., Langer, T., Harder, W., Hartl, F. U., & Veenhuis, M. (1992) *FEBS Lett. 305*, 51−54.
Fayet, O., Louarn, J.-M., & Georgopoulos, C. (1986) *Mol. Gen. Genet. 202*, 435−445.
Fenton, W. A., Kashi, Y., Furtak, K., & Horwich, A. L. (1994) *Nature 371*, 614−619.
Fisher, M. T. (1992) *Biochemistry 31*, 3955−3963.
Fisher, M. T. (1994) *J. Biol. Chem. 269*, 13629−13636.
Flynn, G. C., Beckers, C. J. M., Baase, W. A., & Dahlquist, F. W. (1993) *Proc. Natl. Acad. Sci. U.S.A. 90*, 10826−10830.
Georgopoulos, C. P., & Welch, W. J. (1993) *Annu. Rev. Cell Biol. 9*, 601.
Georgopoulos, C. P., Hendrix, R. W., Casjens, S. R., & Kaiser, A. D. (1973) *J. Mol. Biol. 76*, 45−60.
Gething, M. T., & Sambrook, J. (1992) *Nature 355*, 33−45.
Hames, B. D. (1981) in *Gel Electrophoresis of Proteins: A Practical Approach* (Hames, B. D., Rickwood, D., Eds.) pp 1−18, IRL Press Limited, Oxford, U.K.
Hayer-Hartl, M. K., Ewbank, J. J., Creighton, T. E., & Hartl, F. U. (1994) *EMBO J. 13*, 3192−3202.
Hemmingsen, S. M., Woolford, C., et al. (1988) *Nature 333*, 330−334.
Hendrix, R. W. (1979) *J. Mol. Biol. 129*, 375−382.
Hohn, T., Hohn, B., Engel, A., Wurtz, M., & Smith, P. R. (1979) *J. Mol. Biol. 129*, 359−373.
Horowitz, P. M., Hua, S., & Gibbons, D. L. (1995) *J. Biol. Chem. 270* (4), 1535−1542.
Ishii, N., Tagushi, H., Sumi, M., & Yoshid, M. (1992) *FEBS Lett. 299*, 169−174.
Jones, D. E., Jr., Brennan, M. D., Hempel, J., & Lindahl, R. (1988) *Proc. Natl. Acad. Sci. U.S.A. 85*, 1782−1786.
Laemmli, U. (1970) *Nature 227*, 680−685.
Landry, S. J., Jordan, R., McMacken, R., & Gierasch, L. M. (1992) *Nature 355*, 455−457.
Landry, S. J., Zeilstra-Ryalls, J., Fayet, O., Georgopoulos, C., & Gierasch, L. M. (1993) *Nature 364*, 255−258.
Lathe, R., Skory, S., & Kieny, M. P. (1984) *BRL Focus 6*, 1−6.
Martin, J., Langer, T., Boteva, R., Schramel, A., Horwich, A. L., & Hartl, F. U. (1991) *Nature 352*, 36−42.
Mendoza, J. A., Bulter, M. C., & Horowitz, P. M. (1992) *J. Biol. Chem. 267*, 24648−24654.
Novick, R. P., Adler, G. K., Majumder, S., Khan, S. A., Carleton, S., Rosenblum, W. D., & Iordanescu, S. (1982) *Proc. Natl. Acad. Sci. U.S.A. 79*, 4108−4112.
Popa, M. (1988) Ph.D. Thesis, University of Pittsburgh.
Richarme, G., & Kohiyama, M. (1994) *J. Biol. Chem. 269*, 7095−7098.
Saibil, H., Dong, Z., Wood, S., & Auf der Mauer, A. (1992) *Nature 353*, 25−26.
Tilly , K., Murialdo, H., & Georgopoulos, C. (1981) *Proc. Natl. Acad. Sci. U.S.A. 78*, 1629−1633.
Todd, M. J., Viitanen, P. V., & Lorimer, G. H. (1993) *Biochemistry 32*, 8560−8567.
Todd, M. J., Viitanen, P. V., & Lorimer, G. H. (1994) *Science 265*, 659−665.
Viitanen, P. V., Lubben, T. H., Reed, J., Goloubinoff, P., O'Keefe, D. P., & Lorimer, G. H. (1990) *Biochemistry 29*, 5665−5671.
Viitanen, P. V., Gatenby, A. A., & Lorimer, G. H. (1992) *Protein Sci. 1*, 363−369.
Weissman, J. S., Kashi, Y., Fenton, W. A., & Horwich, A. L. (1994) *Cell 78*, 693−702.
Xie, Z. (1994) Ph.D. Thesis, University of Pittsburgh.
Xie, Z., & Hendrix, R. W. (1995) *J. Mol. Biol.* (in press).
Zahn, R., Spitzfaden, C., Ottiger, M., Wuthrich, K., & Pluckthun, A. (1994) *Nature 368*, 261−265.

BI951348N